Journal of Ceramic Processing Research. Vol. 18, No. 2, pp. 137~140 (2017)

J O U R N A L O F
Ceramic Processing Research

Thermodynamic analysis and phase characterization of hercynite with TiO_2 addition

Mingwei Yan, Yong Li*, Junhong Chen, Shanghao Tong and Haixia Qin
School of Materials Science and Engineering, University of Science and Technology Beijing, Beijing 100083, China

Analytically pure Fe_2O_3, Al_2O_3 and TiO_2 were used as raw materials, batched in the TiO_2: Fe_2O_3: Al_2O_3 mass ratio of 0: 44: 56 and 2: 44:56, respectively, and pressed into specimens with size of Φ25 mm × 30 mm. The green specimens were fired in a CO_2 and CO mixing atmosphere at 1550 °C for 6hrs. The fired specimens were characterized by XRD, Rietveld refinement, SEM, EDS, and XPS to investigate the existing state of TiO_2 in the synthesized specimens. The results show that after firing at 1550 °C for 6 hrs, the specimen added with TiO_2 has a homogeneous structure and $^{IV}(Fe_{0.837}Al_{0.163})_{\sum 1.000}{}^{VI}(Fe_{0.180}Al_{1.764}Ti_{0.034})_{\sum 1.978}O_{\sum 4000}$ as its phase. The introduced TiO_2 participates in the synthesis reaction of hercynite and enters into crystal lattices of hercynite in the form of Ti^{4+}. Ti^{4+} occupies the tetrahedron and octahedron positions, increasing the lattice constant.

Key words: Structure, Hercynite, Tetrahedron, Octahedron, $^{IV}(Fe_{0.837}Al_{0.163})_{\sum 1.000}{}^{VI}(Fe_{0.180}Al_{1.764}Ti_{0.034})_{\sum 1.978}O_{\sum 4000}$.

Introduction

Spinel type transition metal oxides is a class of chemically and thermally stable materials, which belong to double oxides (AB_2O_4) containing interstitial metal cations in lattice sites and possess two distinct types of symmetry with respect to the oxygen anions: tetrahedral and octahedral [1, 2]. Spinels with their B cations in octahedral sites (and A cations in trtrahedral sites) are classified as normal spinels. Those with their A cations only in octahedral sites are classified as inverse spinels. Due to their high melting temperature and low thermal conductivity, spinels are applied as protective coatings against chemical attack from fused metal or glass [3]. Among these spinels, hercynite ($FeAl_2O_4$) is paid widely attention because it combines the excellent physical and chemical properties and has high ductility (fracture-mechanical strength) and flexibility against cracking and spalling [4]. Therefore it is a promising candidate substituting for magnesia chrome brick used at the burning zone of dry-method cement rotary kilns [5-7]. Therefore preparation of $FeAl_2O_4$ is gaining importance. Amirkhanyan *et al.*[8] discuss the possibility of hercynite formation at the interface of a ceramic Al_2O_3 based filter and a metallic melt based on ab initio density function theory calculations. The result showed that the formation of hercynite through reactive FeO was more likely. Since the oxygen partial pressure scope for FeO stable existence is very narrow [9], the inappropriate control of atmosphere will result in the formation of metal Fe or Fe_2O_3, and consequently lead to the impurities of metal Fe, hematite and corundum in the products [7, 10]. Therefore, synthesis of hercynite with high purity is always the key issue for industrial mass production and practical application.

Up to now, various methods including reactive plasma sparying [2], reaction sintering [7], pulsed laser ablation [11] and radial combustion of Fe_2O_3/aluminum thermite [12] etc. have been adopt to synthesize hercynite. Among these methods, addition of sintering agents is found to be an effective one to produce hecynite with high purity. Usually the additives are TiO_2 and SiO_2 [13, 14]. Although the introduction of SiO_2 promotes the formation of hecynite, too much SiO_2 will decline the hot properties of the bricks remarkably. By contrast, TiO_2 has better influences on the hot properties of magnesia materials. Ma *et al.*[14] investigated the effect of TiO_2 on the synthesis of hercynite using Fe_2O_3, α-Al_2O_3 and graphite as raw materials sintered at 1400-1550 °C in high-purity nitrogen atmosphere. The result showed that TiO_2 could generate a simulative significance on hercynite formation. Besides Ghanbarnezhad *et al.* [15] reported addition of TiO_2 improved such properties as the coating ability and corrosion resistance of magnesium aluminate spinel bricks. No further investigation of the effect of TiO_2 on synthesis of hecynite both from theoretical and experimental aspects is carried out. In this work, hecynite was prepared using reaction sintering method. TiO_2 was introduced to promote the sintering. Based on Rietveld refinement of the XRD powder pattern, SEM with EDS and XPS, the existing state of TiO_2 in hecynite was discussed.

Experimental Procedure

Analytically purity of Fe_2O_3 ($\omega(Fe_2O_3) > 99.2\%$),

*Corresponding author:
Tel : +86-10-6233-2666
Fax: +86-10-6233-2666
E-mail: lirefractory@vip.sina.com

Al_2O_3 (ω (Al_2O_3) > 99.5%) and analytically purity TiO_2 ($\omega(TiO_2)$ > 99.3%) were used as raw material with dextrin as the binder. The starting powders ($x = \omega(TiO_2)/\omega(FeO + Al_2O_3)$) with different x values (x = 0.02) (numbered as A_0 and A_1) were wet milled in a planetary ball miller with ethyl alcohol as the grinding medium. After ball milling at 500rpm for 48hrs, the slurry was dried in air and pressed into specimens with size of Φ25 mm × 35 mm under the pressure of 10MPa. Then the specimens were put into a tube furnace and fired at 1550 ºC for 6 hrs in a controllable CO_2 and CO mixing atmosphere.

The phase composition of the specimen after reaction was characterized by X-ray diffraction on a Rigaku D/Max 2200PC diffractometer (RigakuCorp., Tokyo, Japan) adopting CuKα(λ = 1.5418 Å) with the maximum power of 18KW from 10° to 140 º with the scanning time of 120 min. XRD refinement of specimen A_1 was carried out using TOPAS software based on the Rietveld refinement theory. The microstructure of the specimens after reaction was observed by a scanning electronic microscope (Quanta200, FEI, Holland) equipped with an energy dispersive spectrometer (INCA250 Oxford Instrument, UK). The oxidation state of Ti was determined from X-ray photoelectron spectroscopy analysis (AXIS ULTRA^{DLD}).

Results and Discussion

Theoretical analysis

Considering the valence state of Fe and Ti may change during the synthesis process, the existing state of TiO_2 is important to estimate for the synthesis and microstructure of hecynite. At high temperature and low oxygen partial pressure, the reduction reactions of TiO_2 can be expressed in the form of oxygen potential state as follows [16].

$$6TiO_2(s)=2Ti_3O_5(s)+O_2(g)$$
$$\Delta G_1=778220-225.64T+RT\ln\frac{Po_2}{P^\theta} \quad (1)$$
$$\lg\frac{Po_2}{P^\theta}=\frac{225.64}{2.303R}-\frac{778220}{2.302RT}$$

$$4Ti_3O_5(s)=6Ti_2O_3(s)+O_2(g)$$
$$\Delta G_2=778220-169.84T+RT\ln\frac{Po_2}{P^\theta} \quad (2)$$
$$\lg\frac{Po_2}{P^\theta}=\frac{169.84}{2.303R}-\frac{778220}{2.302RT}$$

$$2Ti_2O_3(s)=4TiO(s)+O_2(g)$$
$$\Delta G_2=952260-156.48T+RT\ln\frac{Po_2}{P^\theta} \quad (3)$$
$$\lg\frac{Po_2}{P^\theta}=\frac{156.48}{2.303R}-\frac{952260}{2.302RT}$$

$$2TiO(s)=2Ti(s)+O_2(g)$$
$$\Delta G_4=1005000-165.94T+RT\ln\frac{Po_2}{P^\theta} \quad (4)$$
$$\lg\frac{Po_2}{P^\theta}=\frac{165.94}{2.303R}-\frac{1005000}{2.302RT}$$

In an analogous way, the reduction reactions of Fe_3O_4 can also be expressed in the form of oxygen potential state. It should be pointed out that FeO (wustite) only stably exists above 570 ºC. At high tempearture, Fe_3O_4 possibly participates in the following reactions [16].

$$2Fe_3O_4(s)=6FeO(l)+O_2(g)$$
$$\Delta G_2=978228-458.97T+RT\ln\frac{Po_2}{P^\theta} \quad (5)$$
$$\lg\frac{Po_2}{P^\theta}=\frac{458.97}{2.303R}-\frac{978228}{2.302RT}$$

$$2Fe_3O_4(s)=6FeO(l)+O_2(g)$$
$$\Delta G_6=624682-250.62T+RT\ln\frac{Po_2}{P^\theta} \quad (6)$$
$$\lg\frac{Po_2}{P^\theta}=\frac{250.62}{2.303R}-\frac{624682}{2.302RT}$$

$$2FeO(l)=2Fe(l)+O_2(g)$$
$$\Delta G_7=459400-87.45T+RT\ln\frac{Po_2}{P^\theta} \quad (7)$$
$$\lg\frac{Po_2}{P^\theta}=\frac{87.45}{2.303R}-\frac{459400}{2.302RT}$$

$$2FeO(l)=2Fe(s)+O_2(g)$$
$$\Delta G_7=441410-77.82T+RT\ln\frac{Po_2}{P^\theta} \quad (8)$$
$$\lg\frac{Po_2}{P^\theta}=\frac{77.82}{2.303R}-\frac{441410}{2.303RT}$$

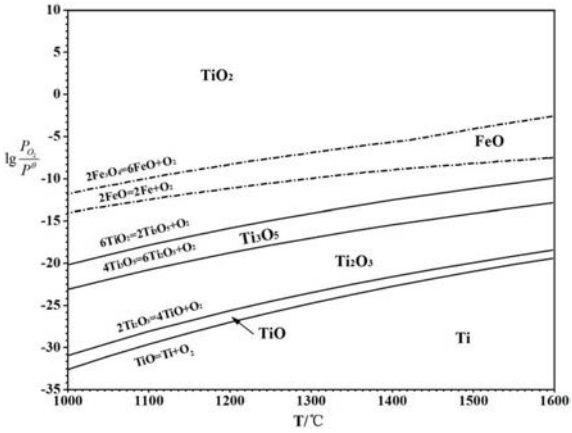

Fig.1. $\lg\frac{P_{O_2}}{P^\theta}$~T curves of Ti-O system containing FeO stable area.

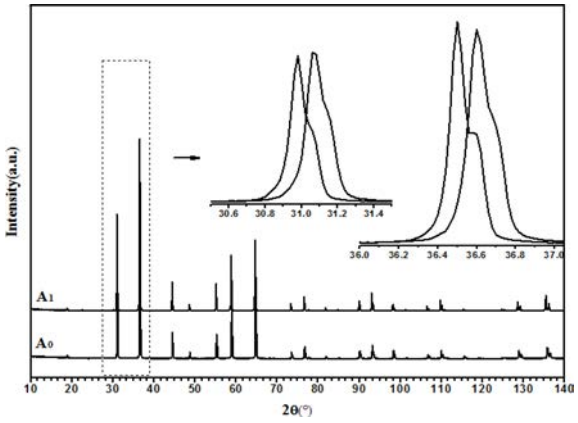

Fig. 2. XRD patterns of fired specimens A_0 and A_1.

$$2FeO(s)=2Fe(l)+O_2(g)$$
$$\Delta G_9=519230-125.10T+RT\ln\frac{Po_2}{P^\theta} \quad (9)$$
$$\lg\frac{Po_2}{P^\theta}=\frac{125.10}{2.303R}-\frac{519230}{2.303RT}$$

$$2FeO(s)+TiO_2(s)=2TiFe_2O_4(s)$$
$$\Delta G_{10}=-33900+5.86T \quad (10)$$

According to the above reactions, the stable state of iron oxide and titanium oxide at the temperature range of 1000-1600 ºC versus $lg\frac{Po_2}{P^\theta}$ is shown in Fig. 1. It can be seen that the stable area of FeO is within that of TiO_2, indicating that Ti may exist in the form of Ti^{4+} during the hecynite synthesis.

XRD with Rietveld refinement analysis

XRD patterns of the fired specimens A_0 and A_1 are shown in Fig. 2. It can be seen that all the characteristic peaks are corresponding to that of hercynite. Especially for Specimen A_0, it seems that hercynite with high purity may be possible obtained. However it has been pointed out Al_2O_3 particles are enwrapped by hercynite

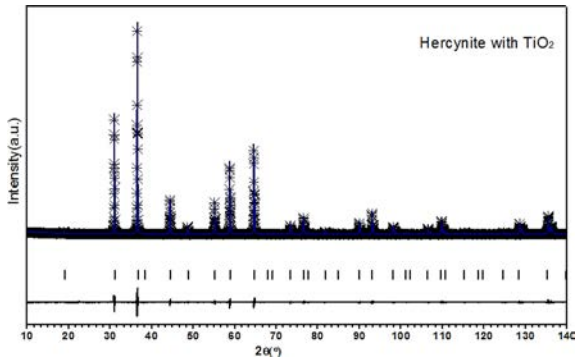

Fig. 3. XRD pattern Refinement result of specimen A_1 (The observed data are indicated by asterisk signs and the calculated profile by the continuous line overlying them. The short vertical lines below the pattern represent the positions of all possible Bragg reflections and the lower curve shows the value of (Y_{io}-Y_{ic}) at each step.).

Table 1. Atom occupancy of hercynite in specimen A_1.

Hercynite with TiO_2 synthesized at 1550 ºC for 6 hrs				
Space group: Fd-3m a = 8.1547 Å; b = 8.1547 Å; c = 8.1547 Å;α = 90.0000 º; β = 90.0000 º; γ = 90.0000 º R-Values: Rwp = 14.11; Rexp = 8.33; Rp = 10.48; GOF = 1.69				
Atom	Atom site			Occupancy
	X	Y	Z	
Fe^{+2}(8a)	0.12500	0.12500	0.12500	0.837
Al^{+3} (8a)	0.12500	0.12500	0.12500	0.163
Fe^{+2} (16d)	0.50000	0.50000	0.50000	0.090
Ti^{+4}(16d)	0.50000	0.50000	0.50000	0.017
Al^{+3}(16d)	0.50000	0.50000	0.50000	0.882
O^{-2} (32e)	0.26330	0.26330	0.26330	1.000

Structural formula:
$^{IV}(Fe_{0.837}Al_{0.163})_{\sum 1.000}{}^{VI}(Fe_{0.180}Al_{1.764}Ti_{0.034})_{\sum 1.978}O_{\sum 4000}$

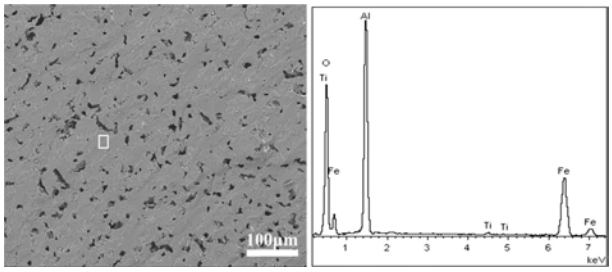

Fig. 4. SEM image and EDS spectrum of facture of specimen A_1.

crystals, which has been confirmed in our recent work [17]. Further analysis shows that the diffraction peaks of Specimen A_1 left shift towards the lower angle, indicating the lattice constant *d*, increases with TiO_2 addition.

For the structure refinement, space group *Fd-3m* was assumed, with the 8(a), 16(d) cation sites and 32(e) oxygen sites fully occupied. Based on the Rietveld theory, the XRD pattern of specimen A_1 was refined by the TOPAS software. The results shown in Table 1 and Fig. 3 indicate that Ti^{4+} enters into the hercynite lattices and occupies the tetrahedron and octahedron positions, which leads to the formation of a complex Ti-hercynite with the general structural formula of $^{IV}(Fe_{0.837}Al_{0.163})_{\sum 1.000}{}^{VI}(Fe_{0.180}Al_{1.764}Ti_{0.034})_{\sum 1.978}O_{\sum 4000}$.

SEM analysis

Fig. 4 shows the SEM image with EDS analysis of the fracture of Specimen A_1. As shown in the SEM image, the hercynite crystal is homogenously distributed and bonded together. EDS spectrum indicates that the element of Ti is contained in hecynite. Combined with the XRD result, it can be proposed that Ti^{4+} possibly diffuses into the hecynite crystal lattices.

XPS Analysis

Fig. 5 is the Ti2p photoelectron spectrum of Specimen A_1, two peaks at Ti2p1/2 458.4eV and Ti2p3/2 464.0eV were observed. According to reference [18, 19], the

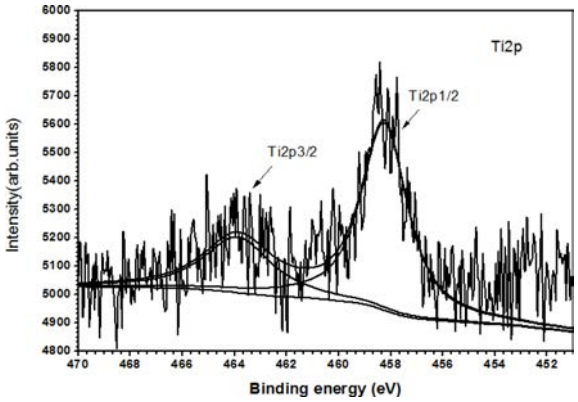

Fig. 5. Ti2p photoelectron spectrum of fired specimen A_1 doped with TiO_2.

valence of titanium is in the form of Ti^{4+}, indicating that Ti^{4+} and Fe^{2+} can coexist and the reduction reaction of Ti^{4+} does not occur as reported in the literature [20]. This is in the agreement with the theoretical calculation and Rietveld refinement analysis.

From above analysis, the effect of TiO_2 on the formation of hecynite can be proposed as follows:

FeO and TiO_2 reacts to form ulvospinel, i.e. $TiFe_2O_4$, which has a 4-2 spinel structure, while hercynite has a 2-3 spinel structure [21-23]. They share the same general structural formula of AB_2O_4. As for $TiFe_2O_4$, A stands Ti^{4+} and B is Fe^{2+}. In view of hercynite, A is Fe^{2+} and B stands Al^{3+}. At high temperatures, A and B ions disorderedly distribute in octahedron and tetrahedron positions and the balance equation can be expressed as following:

$$A_{tet} + B_{oct} = A_{oct} + B_{tet} \quad (11)$$

The general structural formula can be expressed as $(A_{1-x}B_x)(A_xB_{2-x})O_4$, where x is the inversion parameter. Since ulvospinel and hercynite both belong to spinels, they can form a homogenous solid solution phase [24] which has been verified in Fig. 4. Based on the Rietveld refinement analysis, the structure formula of hecynite formed in this experiment can be expressed as ${}^{IV}(Fe_{0.837}Al_{0.163})_{\sum 1.000}{}^{VI}(Fe_{0.180}Al_{1.764}Ti_{0.034})_{\sum 1.978}O_{\sum 4000}$. The radius of the octahedron ions in the order from small to large is as follows: $Al^{3+}(0.530) < Ti^{4+}(0.605) < Fe^{2+}(0.645)$ [24]. Therefore introduce of Ti^{4+} into the octahedron positions of hercynite crystal lattice will increase the lattice constant, which is verified by XRD analysis.

Conclusions

Analytically pure Fe_2O_3 ($\omega(Fe_2O_3) > 99.5\%$), Al_2O_3 ($\omega(Al_2O_3) > 99.3\%$), and TiO_2 ($\omega(TiO_2) > 99.5\%$) were used as raw materials, batched in the TiO_2: Fe_2O_3: Al_2O_3 mass ratio of 0: 44: 56 and 2: 44:56 respectively, added with dextrin as the binder, pressed into green specimens, and heat treated at 1550 °C for 6 h. The fired specimens added with TiO_2 has a homogeneous structure and the main phase is a complex spinel ${}^{IV}(Fe_{0.837}Al_{0.163})_{\sum 1.000}{}^{VI}(Fe_{0.180}Al_{1.764}Ti_{0.034})_{\sum 1.978}O_{\sum 4000}$. The introduced TiO_2 participates in the synthesis reaction of hercynite and enters into crystal lattices of hercynite in the form of Ti^{4+}. Ti^{4+} occupies the tetrahedron and octahedron positions, increasing the lattice constant.

References

1. S.E. Ziemniak, R.A. Castelli, J. Phys. Chem. Solid 64 (2003) 2081-2091.
2. Y. Yang, D.R. Yan, Y.C. Dong, X.G. Chen, L. Wang, Z.H. Chu, J.X. Zhang, J.N. He, J. Alloys. Compd. 579 (2013) 1-6.
3. G. Lallemand, S. Fayeulle, D. Treheux, J. Eur. Ceram. Soc. 18 (1998) 2095-2100.
4. D.P. Duttaa, G. Sharmab, Mater. Sci. Eng. B 176 (2011) 177-180.
5. G.P. Liu, N.L, W. Yan, G.H. Tao and Y.Y. Li, J. Ceram. Process. Res. 4 (2012) 480-485.
6. G.P. Liu, N. Li, W. Yan, G.H. Tao, W. Zhou, Y.Y. Li, Ceram. Int. 40 (2014) 8149-8155.
7. J.H. Chen, L.Y. Yu, J.L. Sun, Y. Li, W.D. Xue, J. Eur. Ceram. Soc. 31 (2011) 259-263.
8. L. Amirkhanyan, T. Weissbacha, J. Kortus, C.G. Aneziris, Ceram. Int. 40 (2014) 257-262.
9. C.E. Meyers, T.O. Mason, W.T. Petuskey, J.W. Halloran, H.K. Bowen, J. Am. Ceram. Soc. 63 (1980) 659-663.
10. P.M. Botta, E.F. Aglietti, J.M. Porto. Mater. Chem. Phys. 76 (2002) 104-109.
11. G.A.C. Rodriguez, G.G. Guilluen, M.I.M. Palma, T.K.D. Roy, A.M.G. Hernandez, J. Appl. Ceram. Technol. 12 (2015) E34-E43.
12. L. Durães, B.F.O. Costa, R. Santos, A. Correia, J. Campos, A. Portugal, Mater. Sci. Eng. A. 465 (2007) 199-210.
13. S.L. Ma, Y. Li, Y.J. Li, Z.F. Wang, W.B. Xia, F. Ma, Z.H. Huang, Naihuo Cailiao (Chinese Version) 47(2013) 161-165.
14. S.L. Ma, Y. Li, J.L. Sun, Z.F. Wang, Naihuo Cailiao (Chinese Version) 44 (2010) 409-412.
15. S. Ghanbarnezhad, A. Nemati, M. Bavand-Vandchali, R. Naghizadeh, J. Chem. Eng. Mater. Sci. 4 (2013) 7-12.
16. Y.Z. Chen, Chemical Thermodynamics of Refractories Beijing Metallurgical. Industry. Press. 655 (2001) 394-396.
17. J.H. Chen, M.W. Yan, J.D. Su, B. L, J.L. Sun, K.C. Zhou, X.M. Hou, J. Ceram. Soc. Jpn. 123 (2015) 595-600.
18. S. Hasimoto, A. Tanaka, Surf. Interface. Anal. 34 (2002) 262-265.
19. http://www.lasurface.com/database/elementxps.php
20. Y. Wu, X. Wu and S. Qin, J. Solid. State. Chem. 185 (2012)72-75.
21. M.J. Rossiter, P.T. Clarker. Nat. 207 (1965) 402.
22. M. Sorescu, T. Xu, A. Wise, M. Díaz-Michelena, M.E. McHenry, J. Magn. Magn. Mater. 324 (2012) 1453-1462.
23. L. Larsson, H.S.C. O'Neill, H. Annersten, Eur. J. Mineral. 6 (1994) 39-51.
24. J. Hauck, J. Solid. State. Chem. 36 (1981) 52-65.